

LETTER OF INTENT
FOR
A TEVATRON COLLIDER BEAUTY FACTORY

J. T. Volk, P. M. Yager
University of California at Davis, Davis, CA

R. Edelstein
Carnegie Mellon University, Pittsburgh, PA

D. Christian
Fermilab, Batavia, IL

B. Lundberg, N. W. Reay*, K. Reibel, R. A. Sidwell, N. Stanton
Ohio State University, Columbus, OH

G. R. Kalbfleisch, P. Skubic, J. Snow, S. E. Willis
Oklahoma University, Normal, OK

4-MAR-87

* Spokesperson

TABLE OF CONTENTS

<u>SUBJECT</u>	<u>PAGE</u>
<u>INTRODUCTION AND PHYSICS</u>	3
Lifetimes and conventional decay modes	3
Mass-mixing	4
Searching for $B \rightarrow u$	5
CP violation	5
<u>DETECTOR DESIGN CRITERIA</u>	7
General collider event characteristics	7
Selection of trigger electrons	8
<u>DETECTOR LAYOUT</u>	9
<u>DETECTOR PERFORMANCE</u>	10
Impact parameter resolution	10
Momentum resolution, production angle resolution and mass-fitting	11
Efficiency for fitting neutral pions and "vees"	12
<u>TRIGGERING</u>	12
Level 1	12
Level 2	13
Level 3	13
<u>SUMMARY</u>	14
<u>PRELIMINARY COST ESTIMATES</u>	15
<u>POSSIBLE LOCATION</u>	16
<u>PRELIMINARY TIME SCHEDULE</u>	16
<u>REFERENCES</u>	17
<u>FIGURES</u>	18

A TEVATRON COLLIDER BEAUTY FACTORY

A hadron collider beauty production experiment which will increase our knowledge of mixing, rare decay modes and even of CP violation could be performed using a new type of detector at the upgraded Fermilab Tevatron. In order to progress from the hundreds of thousands of $B\bar{B}$ events which can be tagged per year at a luminosity of several times 10^{29} /cm²-sec to an ultimate yield of tens of millions at a luminosity of several times 10^{31} /cm²-sec, we also must embark on a learning curve which will take many years and will require development both of hardware and software before achieving a final system. A new high-luminosity intersection region would have to be included as part of the presently-planned Tevatron Collider upgrade. Designing and constructing an initial system will take four years. Thus, in the light of the positive decision on the SSC, a start must be made soon if Fermilab is ever to play a strong role in this exciting area of physics.

Designing even the initial system will require several man-years of effort by a dedicated group of people, together with concurrent work in prototyping and testing. We therefore ask that the Physics Advisory Committee give us their opinion of the priority such a project should be given at Fermilab, within the context that eventually it will require a devoted interaction region which accesses the full achieved luminosity of the machine.

Initially, we discuss physics accessible as the $B\bar{B}$ yield increases. Subsequently, we outline a detector which can be staged, increasing its power (and cost) as we progress along our learning curve. Finally, costs and time schedules are estimated for the initial version of this detector and possible locations are discussed.

THE PHYSICS OF BEAUTY:

Beauty physics which can be accessed depends sharply on the number of reconstructed ("fit") events. Present and even planned fixed-target experiments at best can fit hundreds of decays, the TPC at PEP at best thousands. LEP experiments are severely limited in the study of beauty physics because of the large diameter of their vacuum pipes. The SLD detector running for 10^7 seconds/year at 6×10^{30} /cm²-sec luminosity on the Z^0 could record 260,000 $B\bar{B}$ events per year, less than a hundred thousand of which would be equally suitable for fitting as the ones selected in the Tevatron experiment described below. Therefore, it is important to discuss physics as a function of fit events, and to point out where the higher yield of the Tevatron permits access to new areas.

Lifetimes and conventional decay modes:

At present, indirect measurements of the B lifetime (averaged over particle type) exist, as do measurements for several of the normal $b \rightarrow c$ branching ratios. Limits at

the few percent level exist for the ratio of $b \rightarrow u$ / $b \rightarrow c$ transitions using the higher momentum end-point for decay leptons expected from charmless decays, but this technique appears to have reached its limit in sensitivity.

As the yield of relativistically-boosted and mass-fit Beauty decays increases into the hundreds, direct measurements of lifetimes will be made and these will be separated into charged versus neutral modes; some baryons and excited states also should be discovered. As the yield increases into the thousands, lifetimes will become available as a function of particle type and normal $b \rightarrow c$ modes can be studied adequately for a variety of particle types.

Extrapolating from the MARK III results for charm, as the fit $B\bar{B}$ yield climbs into the 10^4 region, the Cabibbo-suppressed decays which give information on the presence or absence of various weak-decay diagrams (exchange, annihilation, etc.) will become accessible. Beauty events, with their four decay vertices, have a more complicated topology than for charm alone and hence a lower fitting efficiency. Because of this, several hundred thousand relativistically boosted events are required on tape to attain a statistical power in the beauty sector equivalent to that of the tens of thousands of charm events measured by MARK III.

Mass mixing:

Neutral beauty decay mixing can be studied by noting the ratio of same- to opposite-sign semi-leptonic decays found for an initially associatively-produced $B\bar{B}$ system. The relative yield of of right-sign (e.g. $B \rightarrow \mu^-$) and wrong-sign (e.g. $B \rightarrow \mu^+$) decays is given below as a function of the decay rate Γ and the mass difference δm :

$$\text{RIGHT} = (e^{-\Gamma t}) [1 + \cos(\delta m t)]$$

$$\text{WRONG} = (e^{-\Gamma t}) [1 - \cos(\delta m t)]$$

For small $(\delta m/\Gamma)$, as is shown in figure 1, wrong-sign decays peak near two lifetimes and systematics can be improved by observing the ratio of wrong- to right-sign decays beyond several lifetimes. For example if $\delta m/\Gamma < 0.25$, beyond 3.5 lifetimes the number of right-sign decays is reduced by 33 while 31% of wrong-sign decays are retained. This mode of operation is not accessible for machines which produce slowly-moving B's.

It is essential to remove $b \rightarrow c \rightarrow \text{lepton}$ channels, as they give a false wrong-sign signal. Finally, B_d decays are expected to have a $(\delta m/\Gamma)$ of perhaps 10%, whereas this ratio is expected to be more like 0.5 for the B_s mesons which will occur in approximately 20% of the data sample. Before mixing can be studied adequately, it must be ascertained whether the wrong-sign decay is from a B_d or B_s parent. This can be done using particle identification (which can easily be included as an upgrade

to the present minimal design) and by observing mass differences for fit decays. The addition of these latter requirements moves the number of $B\bar{B}$ events required on tape in order to fully examine mixing well into the 10^5 range.

Neglecting for the moment the use of beauty as a tag for heavier objects, unless there are unexpected surprises, at full luminosity SLD in the beauty sector can hope to repeat the success of MARK III in the charm sector and may be able to examine mixing.

Searching for $b \rightarrow u$:

Currently, the most pressing problem for beauty is the existence (and size of) the $b \rightarrow u$ branching ratio. As mentioned previously, the end-point method has reached its limit of sensitivity and exclusive decay channels must now be examined for evidence of this elusive transition. The $B \rightarrow \tau$ mode is often cited as the method of choice, but its branching ratio is expected to be small (10^{-5}) and the final state is topologically difficult to identify. Theorists have suggested the study of $b \rightarrow u$ modes containing charm in the final state and have even suggested that observation of a charmless final state is insufficient evidence for the $b \rightarrow u$ mode because of the possibility of W-boson loop diagrams.¹ Most of the many possible $b \rightarrow u$ decay modes containing charm are expected to be at the 10^{-4} level, and access would require a million $B\bar{B}$ events on tape. The following are some typical decay topologies for these channels:

$$B_{d,u} \rightarrow F^+ X_{c=0,s=0} \text{ or } DX_{c=0,s=1},$$

which include exclusive channels like:

$$B_u^+ \rightarrow F^+ \pi^0, F^+ \rho^0, F^+ \pi^+ \pi^-, F^+ \phi, F^+ K^+ K^-, \\ F^+ \eta_8, F^+ \eta_0, F^+ \eta_c, F^+ J/\psi, \text{ etc.}; D^0 K^+, \\ D^+ K^0, D^{*0} K^+, D^0 K^{*+}, D^{*0} K^{*+}, \text{ etc.}$$

$$B_d^0 \rightarrow F^+ \pi^-, F^+ \rho^-, F^+ \pi^- \pi^0, \text{ etc.}; D^0 K^0, D^{*0} K^0, \\ D^0 K^+ \pi^-, D^{*0} K^{*0}, D^{*0} K^{*0}, \text{ etc.}$$

$$B_s \rightarrow F X_{c=0,s=-1}, \text{ or } DX_{c=0,s=0},$$

which include exclusive channels like:

$$B_s^0 \rightarrow F^+ K^-, F^+ K^{*-}, F^+ \bar{K}^0 \pi^-, \text{ etc.}; \\ D^0 \pi^0, D^0 \eta_8, D^0 \eta_0, D^0 \phi, D^{*0} \phi, D^{*0} \eta_8, \\ D^{*0} \eta_0, D^0 \eta_c, D^0 J/\psi, \text{ etc.}; D^+ \pi^-, D^+ \rho^-, \\ D^+ \pi^- \pi^0, D^{*+} \pi^-, D^{*+} \rho^-, \text{ etc.}$$

CP violation:

Finally, the ultimate goal is the study of CP-violation in the beauty sector. Many authors have discussed such a possibility,^{1,2,3,4,5} which is driven by the unexpectedly long B lifetime. All require non-zero $b \rightarrow u$ decay modes. As CP-violation in the beauty sector is expected to occur in the decay process rather than in the mass-matrix (ϵ' rather than ϵ in the notation of the kaon system), effects may be found both in charged and neutral decays. For the purpose of illustration, let us present in

figure 2 the work of Dunietz and Rosner⁴ for a single neutral decay mode. It is clear that there are striking differences in the dependence on proper decay time for the \overline{B}_S and B_S decays into the same final state ($\overline{D}^0 + \phi$); the former decay is enhanced and the latter suppressed from exponential shape by the presence of CP violation. Unfortunately, the former proceeds through the $b \rightarrow u$ mode which is expected at the 10^{-4} level, while the latter contains a $u \rightarrow s$ contribution and hence is at the 10^{-3} level.

We estimate that 50 fit decays beyond one lifetime based on exponential decay in the latter channel would be sufficient to estimate whether CP suppression below exponential exists at the level of figure 2. Such a decay must be tagged, which requires not only a high- P_T lepton but also something else from the decay partner (e.g. charge, an identified baryon, etc.). Tagging efficiency for the "something else" would be roughly 1/2. The fraction of decays beyond one lifetime is 0.37. The \overline{D}^0 and ϕ each would have an identification efficiency of 1/2. This assumes a mode of analysis in which a ϕ with large impact parameter triggers an exhaustive second pass attempting to identify the \overline{D}^0 as an anti-particle rather than a particle. Such methods were used successfully in a previous emulsion charm experiment (E531), in which over 90% of neutral charm decay vertices were fit. As B_S will be separated from B_d decays to the same final state by mass, accepting 0C \overline{D}^0 events may permit some contamination from the latter mode. The overall efficiency is:

$$\begin{aligned} \text{Efficiency} &= (\text{tag beauty})(\text{tag } \overline{D}^0)(\text{fit } \phi)(\text{beyond one lifetime}) \\ &= 0.046 \end{aligned}$$

The fraction of B's which are strange is taken to be 1/5, and perhaps half of these will be neutral. The number of B's one must have on tape to examine CP violation in this channel is given by

$$\begin{aligned} \text{Number to tag} &= \frac{\text{Number needed}}{(\text{Efficiency})(B_S \text{ fraction})(B.R.)} \\ &= \frac{50}{(0.046)(0.10)(0.001)} \\ &= 11 \text{ million on tape.} \end{aligned}$$

The overall entry level may be somewhat lower because of the large number of accessible interesting decay modes.

There is also the possibility of detecting CP violation in the mass matrix by observing the ratio of wrong-to-right sign decays for B^0 versus \overline{B}^0 mesons:

$$\Gamma(B^0 \rightarrow \text{positive lepton} + X) = \left| \frac{1-\epsilon}{1+\epsilon} \right|^2 e^{-\Gamma t} (1 - \cos \delta m t)$$

$$\Gamma (B^0 \rightarrow \text{negative lepton} + X) = \left| \frac{1+\epsilon}{1-\epsilon} \right|^2 e^{-\Gamma t} (1 - \cos \delta m t)$$

$$\{ [(W/R)_{\overline{B}^0}] / [(W/R)_{B^0}] \} = \left| \frac{1+\epsilon}{1-\epsilon} \right|^4$$

where most of the notation is as for mixing and ϵ is the same CP-violating parameter used in the neutral kaon system. As for mixing, systematics may be reduced considerably by studying wrong-sign decays far out on the lifetime curve. Assuming a theoretical estimate of $\delta m/\Gamma$ for B_d mesons, given 10^7 $B\overline{B}$ events on tape, $\text{Re}(\epsilon)$ could be bounded as being smaller than 0.8% at the 90% CL. Of course, a positive signal at this level would be of considerable interest as standard-model predictions would be violated.

Simply put, it requires several hundred thousand $B\overline{B}$ events on tape to fully examine mixing, over a million to search for the $b \rightarrow u$ mode in particular channels and ten million to gain entry into the world of CP violation in the beauty sector. These rates can be achieved only at high-luminosity hadron colliders.

DETECTOR DESIGN CRITERIA:

General collider event characteristics:

Before discussing the detector, it seems appropriate to present information based on the ISAJET Monte Carlo⁶ for general characteristics of collider events which drive the design. Shown in figure 3 are charged-particle multiplicity distributions both from events containing a $B\overline{B}$ pair and background events which do not contain a $B\overline{B}$ pair. As can be seen, event multiplicity is relatively unaffected by the presence or absence of beauty. The rapidity distribution for the beauty particles themselves (not their decay products) and the rapidity distribution for all other charged particles in the event which do not come from beauty decay are presented in figure 4. From these curves we may infer that a detector subtending an angle of $\pm 23^\circ$ on a single side of an interaction region would contain roughly 1/3 of produced beauty and also 1/3 of the produced charged multiplicity in an interaction. Figure 5 gives gammas for beauty particles produced at angles larger than 45° and less than 20° with respect to the beam direction. It can be seen that only 3% of wide-angle beauty has a gamma in excess of 3, whereas 26% of forward-backward produced beauty has a gamma greater than 6. Results from analysis of charm decays in Fermilab experiments 531 and 653 indicate that increasing the gamma of the parent particle beyond 3-4 both increases the visibility of decay lengths and aids in the determination of impact parameters.

As an aside, the experiment discussed below accesses a range of gamma for beauty of perhaps 6 to 25, a range which is eminently suitable for identification of

hadronic decay tracks. At the same luminosity, a full-energy SSC according to ISAJET would be able to record beauty events at a 4-5 times higher rate, but much of the increase would be in the gamma range 25 to 200 and decay products would be produced forward-backward at small angles with respect to the beam lines. To capture this faster component, a multiple-stage detector would be required and identification of decay hadrons would become more difficult. A Tevatron Beauty factory would, in fact, be competitive with similar ventures at the SSC.

The final piece of general information is that the gamma of a beauty particle and its associated antiparticle appear relatively uncorrelated, as shown in figure 6, but are produced in the same hemisphere.

Selection of trigger electrons:

Now, we wish to turn to more detailed aspects of beauty production which impact on detector design. The goal is to create a design of modest proportions which can be expanded, when the technique is demonstrated, by adding to existing apparatus rather than rebuilding that which already exists. We have therefore chosen to concentrate on an electron trigger, which permits a spatially compact design. In figure 7 we show spectra for electrons satisfying momentum and transverse momentum cuts of 8 GeV/c and 1.2 GeV/c, where P_T is calculated with respect to the beam directions. In the figure, these electrons come from $B \rightarrow e$, $B \rightarrow C \rightarrow e$, $C \rightarrow e$, $\pi \rightarrow e$, $K \rightarrow e$ decays and 1% conversion of gamma rays. It can be seen that electrons from pion and kaon decay have a much steeper dependence on momentum than do the other modes, and can be sharply reduced with a cut of 8 to 12 GeV/c. Though unwanted electrons from gamma conversion appear to have a higher-momentum component than those from pion and kaon decays, their number falls rapidly with increasing P_T and they virtually can be eliminated with a transverse momentum cut of 1.6 to 2.0 GeV/c. Also, with such a cut the background from $C \rightarrow e$ decays is reduced to perhaps 20% of the Beauty signal.

We have chosen to count as acceptable only those associatively produced events in which the beauty particle giving rise to the trigger electron has a relativistic gamma of at least 3 and its partner has a gamma of at least 6. These requirements are driven by the facts that electrons which have significantly more than half of the energy of the parent beauty tend to have reduced impact parameters, and in order both to observe a decay length for and mass fit the beauty partner it must be fast and all its decay tracks must be captured by the apparatus. In figure 8 the effective cross-section in microbarns is shown versus P_T for events in which

- a) The decay from one beauty particle contains a trigger electron with $P > 8$ GeV/c and $P_T > 1.2$ GeV/c;
- b) that beauty particle has a gamma greater than 3;
- c) the gamma of the associated beauty partner (the one not giving rise to the trigger electron) is greater than 6;

- d) the electron and all charged tracks from the associated beauty decay subtend angles between 20 and 400 milliradians with respect to the beam lines. (The justification for this angular acceptance will be given shortly.)

Note that in figure 8, both forward and backward events are folded onto the same plot. Approximately 0.4 microbarns worth of events (1.3% of the total pair-production yield of 30 microbarns) satisfies the above requirements, with most of the loss coming from requiring a stiff, high- P_T semi-leptonic decay. The yield in microbarns for the background electron trigger rate is given in figure 9; for $P_T > 1.4$ GeV/c the rate is entirely dominated by the assumed 1% gamma conversion.

The integrated yield of trigger electrons for events satisfying all but the angle requirements is shown as a function of the production angle in figure 10. Also shown is the fractional number of events where all charged tracks from the accompanying beauty decay are contained within an angle θ . It can be seen that a forward-backward detector with an acceptance of 400 milliradians with respect to the beam directions appears optimal for the above trigger requirements. The fractional number of events in which at least one charged decay track from the partner beauty particle has an angle less than θ is shown in figure 11. It can be seen that for events in which the above trigger is satisfied, 90% of partner beauty decays have no charged decay tracks with an angle less than 20 milliradians.

DETECTOR LAYOUT:

Based on the above trigger requirements, we have fixed upon the detector geometry shown in figure 12. It has a maximum angle of acceptance which varies from 300 milliradians at the far side of an interaction region to 500 milliradians at the near side, and is sensitive to angles greater than 20 milliradians. Several planes of double-sided silicon microstrip detectors are mounted inside a carbon fiber vacuum pipe reinforced with rings, downstream straw-tube chambers are spaced from the silicon by a dipole magnetic field of strength 0.4 GeV/c. The detector is completed with a short electromagnetic calorimeter with a pad segmentation which varies from approximately 1 cm x 1 cm at its innermost edges to 6 cm x 6 cm at its outermost edges.

The entire detector can be contained within a cylinder approximately two meters in length along and 0.8 meters in radius perpendicular to the beam directions. It has an RMS mass resolution which for two-body decay of a beauty particle into charged light decay products varies from 28 MeV in the multiple-scattering limited regime up to 40 MeV for $\gamma_B = 25$. All-charged decays with ≥ 3 prongs have even better resolution and decays with 1-2 neutral pions usually can be fit without degrading resolution below the two-body case given above. Pattern recognition for tracks in general is significantly easier than for present 800 GeV fixed-target hadron-beam experiments.

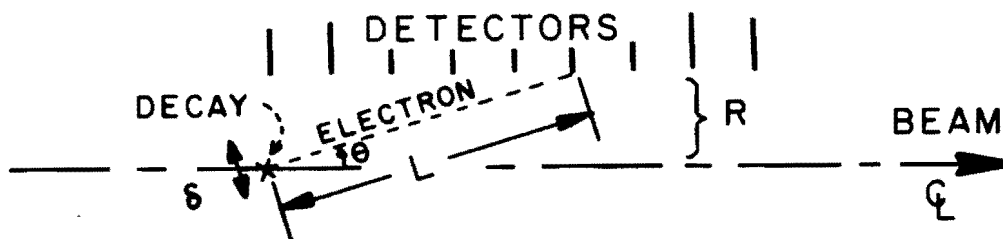
Virtually all of the apparatus can be retained when hadronic and muonic particle

identification systems are added and apparatus for the opposite side of the interaction region can be handled almost as an independent detector. Most of this detector can be built with present-day technology, though a great deal of development would be required for the mechanical mounting of the silicon. The silicon planes closest to the beam would have to be moved out during filling and returned with some degree of accuracy, though tracks could be used to cross-calibrate them with respect to the fixed large-aperture planes. Presently uncertain is the radiation hardness of the integrated microstrip readouts which would be wire-bonded to the outer edges of the silicon, and the possible design of a "thin" tracking transition-radiation detector (TRD) which could be placed upstream of the electromagnetic calorimeter to improve triggering.

DETECTOR PERFORMANCE:

Impact parameter resolution:

As the entire experiment is based on reconstruction of secondary vertices, it is important to demonstrate sufficient spatial resolution at the point of decay. Consider the detector shown below:



θ is the production angle of the decay track, R is the radial distance from the beam axis to the inner edge of the microstrip detectors, L the distance travelled by a decay particle before registering in the first detector and δl the transverse impact-parameter resolution achieved by the detectors in a single view at the point of decay.

$$\theta = \frac{R}{L}$$

The error in theta is dominated by multiple-scattering in the silicon detectors. All detectors used in fitting a track are weighted by their contribution to multiple scattering, which is a complicated process to present in simple form. For pedagogical purposes only, assume that the three 270-micron-thick detectors closest to the interaction are used to find impact parameters. This will give a result similar but slightly inferior to the actual method.

$$\delta\theta = \frac{0.021}{\sqrt{3} P} \sqrt{\frac{X}{X^0}}$$

$$\delta l = L\delta\theta$$

For $X = 0.010 X^0$,

$$\delta l = \frac{(0.0012)R}{P_T}$$

Note that δl is a function of R and P_T only. For $R = 8000$ microns, tracks down to a P_T of 300 MeV/c can be fit with a total radial impact parameter of less than 30 microns.

To set a scale for this number, we note that half of B^0 decay products will have impact parameters less than 300 microns with respect to the primary interaction and half of cascade D^0 decay products will have impact parameters less than 100 microns with respect to the parent Beauty. Impact parameter resolutions better than 28 microns will permit most tracks to be associated cleanly with each of the above three vertices. If the resolution degrades to 60 microns, most of the B decays in the first lifetime will be lost from the required 2-3 standard-deviation cuts on impact parameters, and it will become difficult to distinguish whether tracks come from the parent B or daughter charm decays.

Momentum resolution, production angle resolution and mass-fitting:

Let us now turn to measurement of production angles and charged-track momenta. We have assumed that a typical track passes through 5 planes of double-sided 300-micron-thick silicon microstrip detectors, a 3 mm thick vacuum wall of reinforced carbon fibers, 9 planes of 4 millimeter diameter straw-tube chambers (3 per view) in the center of the magnet and 45 similar planes (5 per view per station) downstream of the magnet. The RMS multiple-scattering angle for the detector is given below:

$$\delta\theta_{\text{Coulomb}} = (1/P) [(0.0022)^2 + (0.0014)^2 + (0.0018)^2]^{0.5} = 0.0032/P$$

where the first, second and third contributions are from the silicon detectors plus vacuum pipe, straw-tube chambers in the magnet and straw-tube chambers downstream of the magnet, respectively. The straw-tube multiple scattering used was the value of $X = 0.001X^0$ achieved for the CLEO and AMY detectors. The precision for measuring production angles is $(0.0022/P)$ radians, which reduces to 4.0×10^{-5} radians for tracks of infinite momentum given the silicon-detector resolution of 8 microns achieved in Fermilab Experiment 653.

Assuming a straw-tube chamber resolution at 4 atmospheres of 50 microns and a magnetic bend of 0.4 GeV/c, the momentum resolution for charged tracks is given by:

$$(\delta P/P) = \{ (0.008)^2 + [(1.2 \times 10^{-4})P]^2 \}^{0.5}$$

For tracks up to 50 GeV/c the momentum resolution is better than 1%. The mass resolution for the worst-case decay into two light charged particles varies from 28 MeV in the multiple-scattering-limited region up to 40 MeV for $\gamma_B = 25$. Almost independently of decay mode, the error in decay angles plays a lesser role than uncertainty in decay momenta in determining mass resolution for the parent Beauty.

Efficiency for fitting neutral pions and "vees":

Though the efficiency for reconstructing neutral pions and "vees" (K_{short} and λ decays) requires considerably more study than presented herein, E653 experience in using a liquid argon detector with similar pad geometry indicates that neutral pions can be reconstructed with efficiencies in excess of 50% for momenta between 3 and 20 GeV/c. The fact that we have almost a meter upstream of the center of the magnet for observing vees, and the high degree of redundancy in the straw chamber system, gives us confidence that we will be able to observe and mass-fit approximately half of charged vees for K_{short} momenta between 3 and 13 GeV/c and λ momenta between 3 and 10 GeV/c. Efficiency for decays at higher momenta would decrease almost linearly with momentum because of the fixed length of the decay region.

TRIGGERING:

Though this design is preliminary, it appears that a triggering algorithm can be developed which can reduce interactions occurring at luminosities in excess of $10^{31}/\text{cm}^2\text{-sec}$ down to a few per second triggers recorded onto tape. When measurement of impact parameters is incorporated into the on-line trigger, on paper there is a $B\bar{B}$ pair in the majority of recorded interactions. Let us now discuss the trigger rate for a luminosity of $10^{31}/\text{cm}^2\text{-sec}$, corresponding to an interaction rate of one megahertz. A multiple-level scheme is proposed, with sufficient fast buffering at each level to minimize losses due to the statistical arrival of data.

Level 1:

We plan to trigger on electrons with $P > 8$ GeV/c using pulse-height in the electromagnetic calorimeter. For P_T greater than 2.0 GeV/c, the magnetic bend affects the radial position of the electron at the calorimeter by less than $\pm 13\%$. Thus, a P_T cut is equivalent to a cut on the product of the shower energy and the radial position of the shower. From figures 8 and 9, for $P > 8$ GeV/c and $P_T > 2.0$ GeV/c and for a detector on a single side of the detector region the trigger rate is 23/second for 1% gamma

conversion and the $B\bar{B}$ yield satisfying all requirements is 1.3 per second. (Figure 8 reads 2.6/second, but it was constructed for the ultimate detector, which would access both sides of the interaction region.) If we have no tracking TRD detector all gammas would be detected in the level 1 trigger, yielding 2300 triggers/second. The initial shower pulse-heights could be accessed in perhaps 100 nanoseconds and a sorting algorithm could be developed which would not take more than 200 nanoseconds. From the triggering standpoint, the proposed detector therefore could handle luminosities above 10^{31} without high-speed event buffering.

Level 2:

For on-line purposes it is sufficient to view straw-tube chambers as strip devices, leaving the attainment of their ultimate resolution for off-line analysis. In figure 10 we see that a minimum electron-angle cut as large as 100 milliradians loses only 10% of events. At such large angles, electrons will suffer less than 1% confusion with other tracks, and reconstruction of an associated track segment in the tube chambers immediately upstream of the electromagnetic calorimeter can be done with bit manipulation in microseconds. Thus, requiring a track in the chamber station immediately upstream of the calorimeter would reduce the trigger rate to 200/second, corresponding to the 8.5% of a radiation length upstream of the calorimeter. Of course, such a reduction could be made in a level 1 trigger were an appropriate tracking TRD to be included.

Within a millisecond, the wide-angle electron track could be traced upstream through most of the silicon, giving a trigger rate of perhaps 15/second. For these purposes the silicon microstrips also would be treated as yes-no devices similar to scintillator hodoscopes.

Level 3:

At this point, timings from off-line ACP analysis of present fixed-target experiments indicate that sufficient tracks could be calculated for the event to yield on-line impact parameters for the electron with an RMS precision of better than 50 microns radially (i.e. for the RMS sum of X and Y transverse views). Such an analysis requires considerable time because many tracks must be reconstructed and the large number of tracks coming from decay vertices must be eliminated before reconstructing the primary point of interaction.. Though subsequent off-line analysis should improve impact-parameter resolution to better than 25 microns, the on-line calculation would be sufficient to permit a two standard deviation cut retaining 70% of the $B\bar{B}$ events while reducing the recorded trigger yield down to an almost pure sample of 1 $B\bar{B}$ event per second satisfying all cuts (including those on the electron impact parameter). Selection on impact parameters also biases against $C \rightarrow e$ decays, which would be reduced to less than 10% of the Beauty signal. Finally, a factor of two increase in beauty yield is possible at the expense of a factor of 5 increase in the level 1 trigger by relaxing approximately 25% on all lepton and γ_B cut requirements.

SUMMARY:

To summarize, based both on experience gained fitting hadronically-produced charm events in present fixed-target experiments and on numbers derived using ISAJET QCD predictions, it appears possible to design a Tevatron experiment which could record onto magnetic tape a high-purity sample of 10^7 $B\bar{B}$ events per year at a luminosity of $10^{31}/\text{cm}^2\text{-sec}$. Though the initial apparatus is less than 2 meters in length and 1.6 meters in diameter, mass resolutions appear to be sufficient to separate B_D and B_S decays to the same final states. Muon and hadron identification could be added after initial running with minimal disturbance to the original system. After considerable experience is gained, apparatus with upgraded design could be added to the other side of the interaction region virtually as an independent detector.

PRELIMINARY COST ESTIMATES:

1)	Silicon detectors, 200 @ \$4000/detector	\$800K
2)	On-board silicon detector electronics, 200,000 channels @ \$2.50/channel.	500K
3)	Silicon mounting, including electronic sensing and development costs.	300K
4)	Straw-tube chambers, 54 planes @ \$2000/plane.	108K
5)	Straw-tube electronics, 20,000 channels @ \$50/channel.	1,000K
6)	Electromagnetic calorimeter, 1500 channels @ \$700/channel (including detector costs)	1,050K
7)	Other data acquisition electronics	500K
8)	Analyzing magnet	800K
9)	operating for the first year assuming a 4 month run and a two month startup.	120K
<hr/>		
	30% contingency on detector and operating alone:	\$1,553K
<hr/>		
	Subtotal, detector and operating:	\$6,731K
10)	Initial interaction region modifications.	?
11)	Upgrades to achieve full Tevatron luminosity.	?

POSSIBLE LOCATION:

Choosing a location at the Tevatron as presently-configured is difficult. Performing shakedown and trigger studies alone for the proposed detector would require at least a full running period. Thus, push-pull arrangements with present collider detectors for a single running period while they are being upgraded do not appear practical.

Exclusive of B0 and D0, only C0 appears to satisfy a reasonable number of requirements, and for that region to be useful both Main Ring and Tevatron abort lines would have to be moved at least one meter. Also, modest initial construction would have to be performed in order to accomodate a detector 2.5 meters in length by 1.6 meters in diameter.

Finally, this intersection region presently has more than a hundred times less luminosity than at B0 and D0. Ultimately, a third low- β system would have to be installed in order to upgrade C0 luminosity. This latter problem in fact is the main reason for the timing of this letter of intent. If plans for a third low β region are not included as part of the Tevatron upgrade, high-statistics studies of Beauty will never become part of the Tevatron repertoire.

PRELIMINARY TIME SCHEDULE:

Given encouragement by the PAC, a full proposal could be developed in time for the 1988 Aspen PAC meeting, as well as performing some initial hardware studies. If approved, the design could be frozen and prototypes constructed for all system elements within a year. Testing of prototypes could be completed in 1989 and full-scale construction could begin provided enhanced funding is in place. A minimum of 30 to 40 scientists divided into six teams would be needed to handle the separate projects of on-line software, off-line analysis, a data acquisition system, the silicon microstrip system, the straw-tube chamber system and the electromagnetic calorimeter. Assuming that a radiation-hard integrated silicon readout becomes available by 1990, as the apparatus is small and redundant it could be constructed in two years, installed and checked out in an additional half year, and be ready for beam by late 1991. The first physics output could occur during 1992-93.

REFERENCES:

- 1) Ling-Lie Chau, Proc. of the 1986 Snowmass SSC Study.
Note that this publication is only the latest in a series by this author dating back several years.
- 2) I. I. Bigi and A. I. Sanda, SLAC-PUB-3879
-3949.
- 3) I. Bigi, SLAC-PUB-4000
-4074.
Note that the above publications by Bigi and Sanda are only the latest in a series going back into the previous decade.
- 4) Isard Dunietz and Jonathan L. Rosner, U. of Chicago Preprint EFI 86-10.
- 5) N. W. Reay, Proc. of the SSC Fixed Target Workshop, 53 (1984).
- 6) ISAJET was designed, constructed and is maintained by Frank E. Paige and Serban D. Protopopescu of Brookhaven National Laboratory. Much of the event-simulation presented herein was taken from N. W. Reay, "ISAJET Study of Beauty Production at TeV I," Ohio State U. Physics Department Report, 1986.

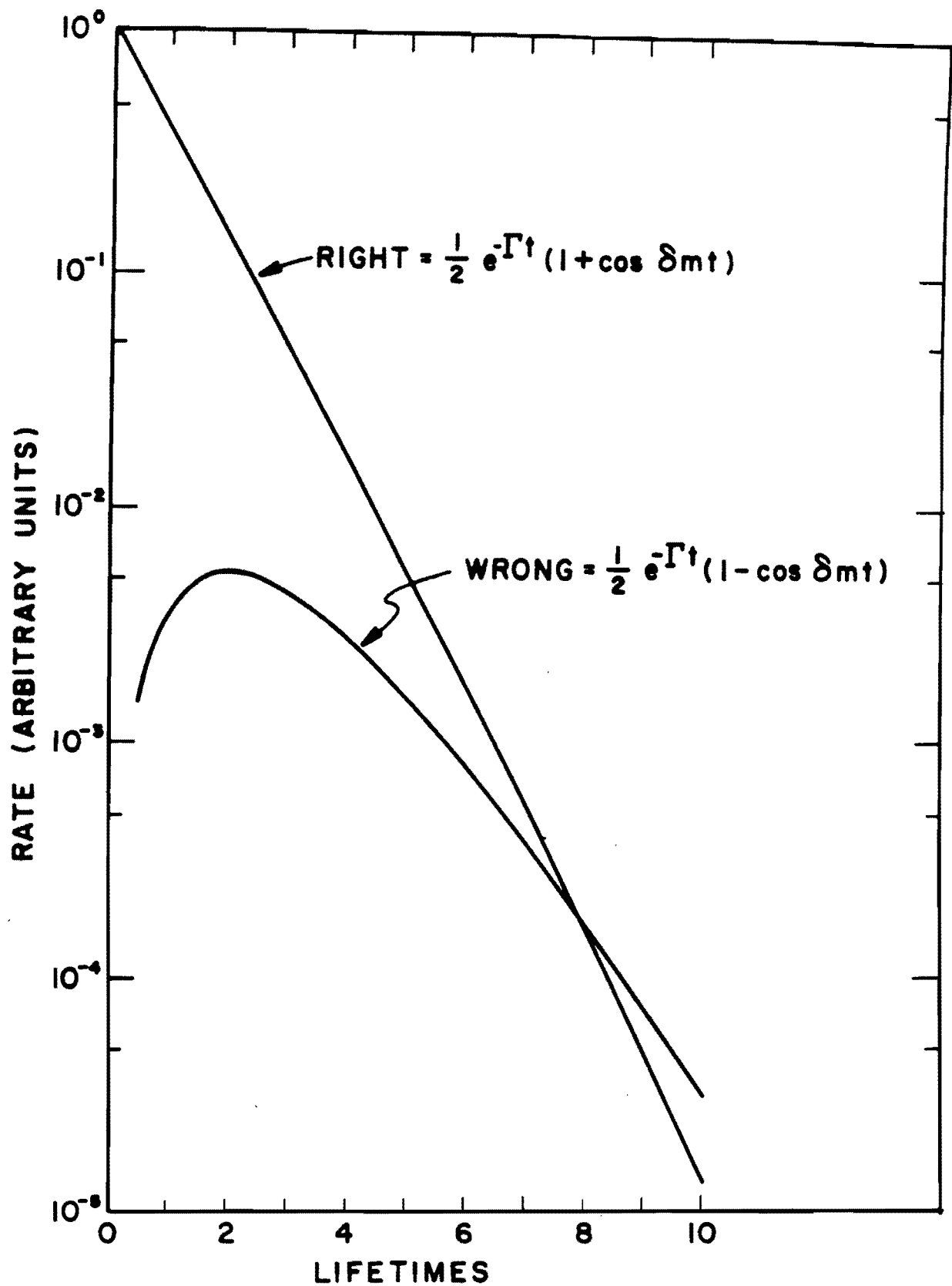


Figure 1 Mass-mixing plotted for $\frac{\delta m}{\Gamma} = 0.2$. Note that wrong - sign decays peak near two lifetimes.

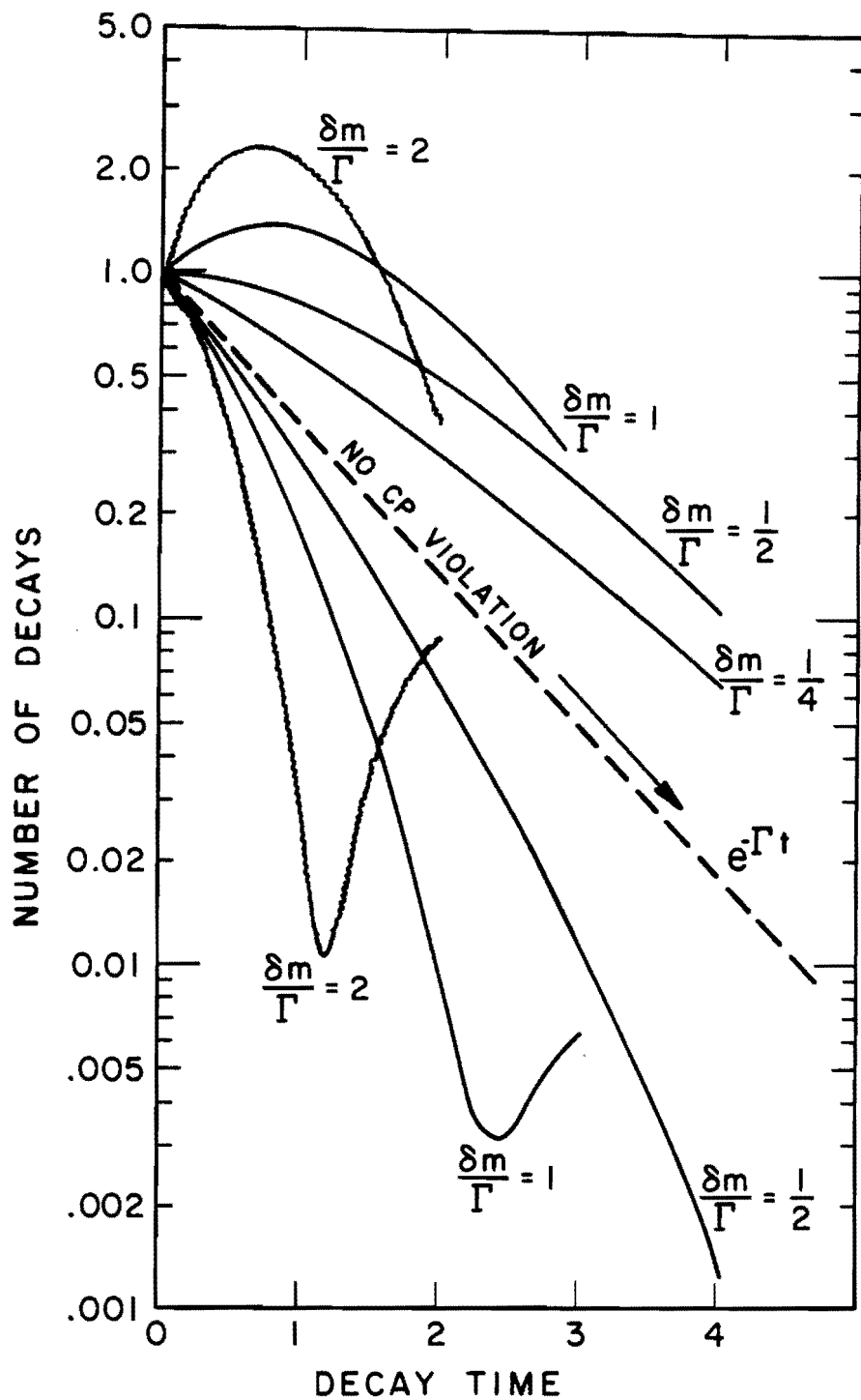


Figure 2 Decay spectra as a function of proper decay time in lifetime units for various values of $\frac{\delta m}{\Gamma}$ for the decays

$$\bar{B}_s^0 \rightarrow \bar{D}^0 + \phi$$

$$B_s^0 \rightarrow D^0 + \phi$$

All curves above the exponential line are for \bar{B}^0 decay, those below are for B^0 decay. The exponential line represents the decay spectrum expected for both cases in the absence of CP violation.

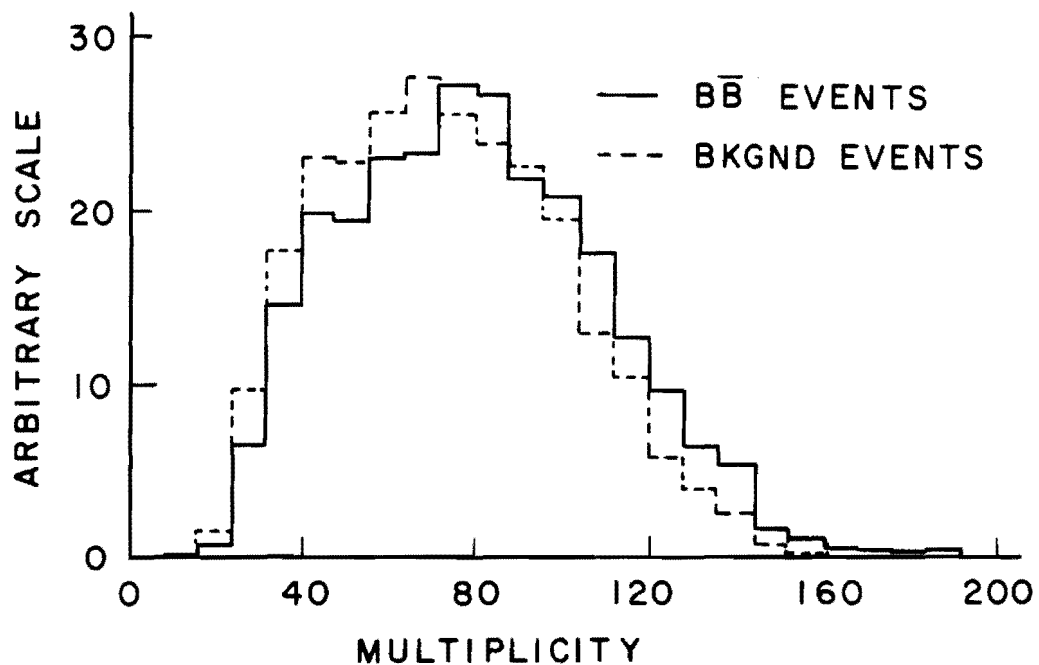


Figure 3 Multiplicity versus number both for events containing B-BBAR pairs and background events which contain neither Beauty nor Charm pairs.

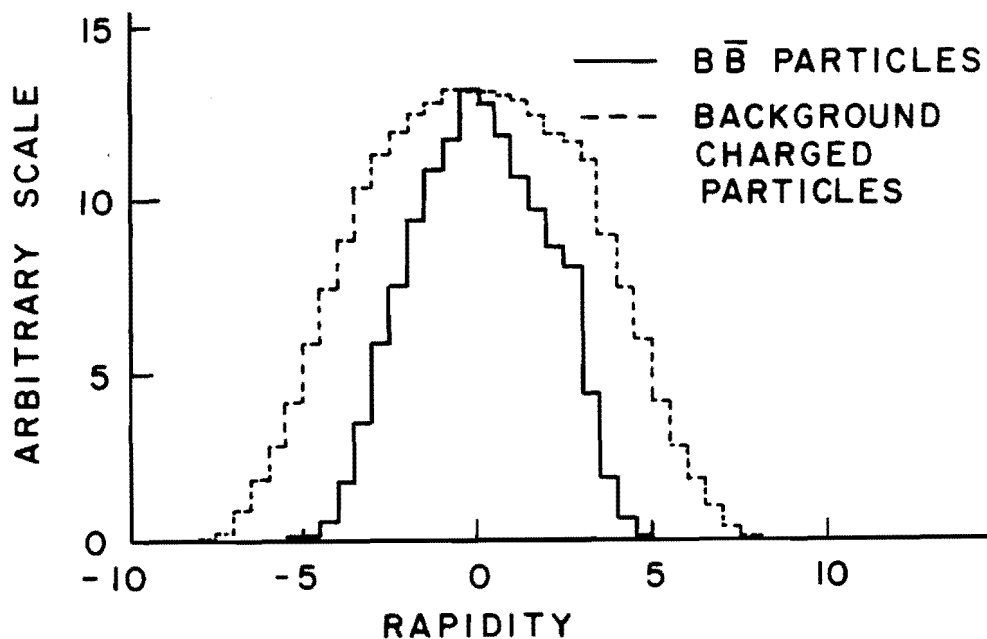


Figure 4 Rapidity of Beauty particles compared to rapidity of charged particles in background events.

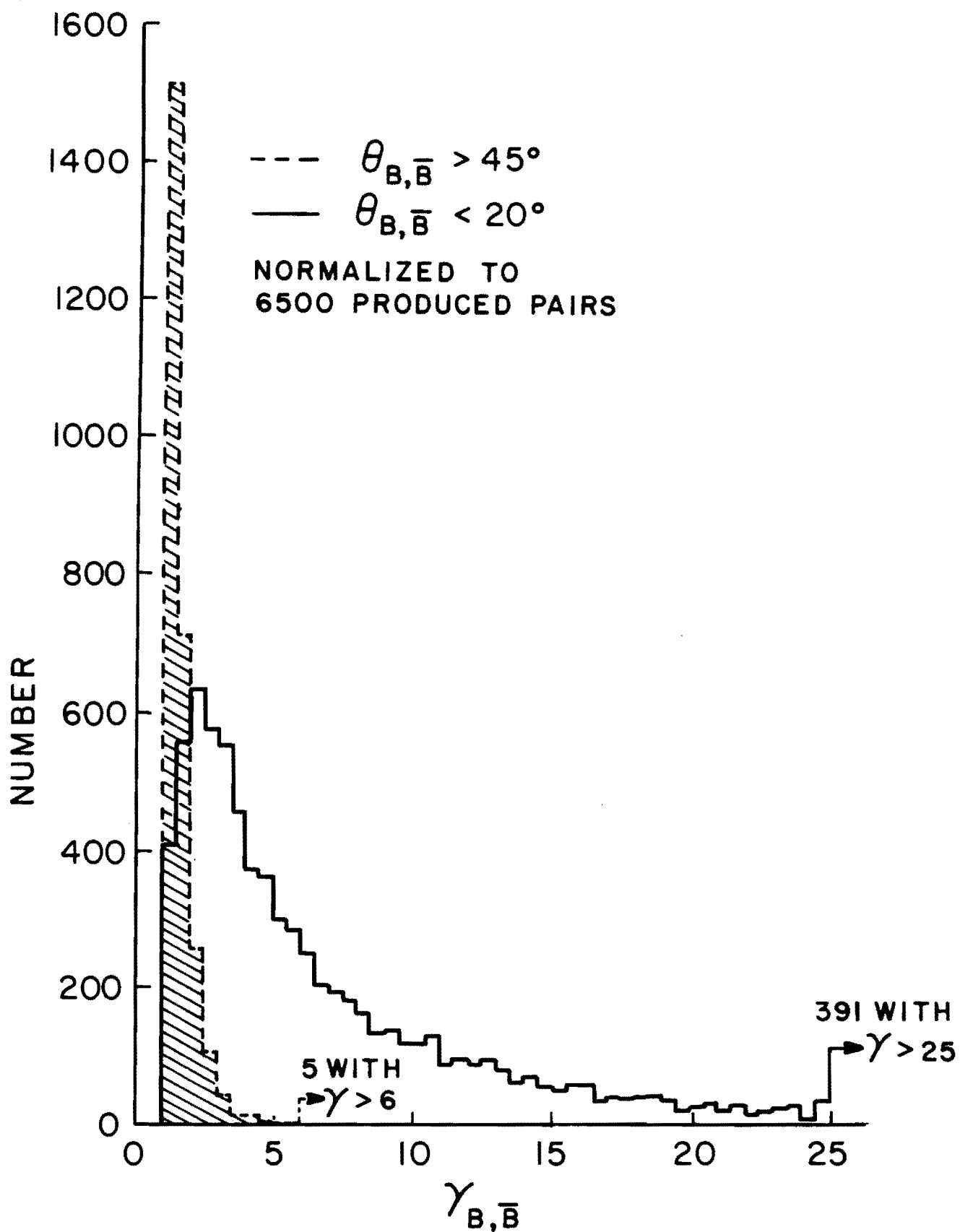


Figure 5 Gammas for beauty particles produced at angles larger than 45 degrees (dashed line) and less than 20 degrees (solid line) with respect to the beam lines (forward and backward directions were folded into the angular range 0 to 90 degrees).

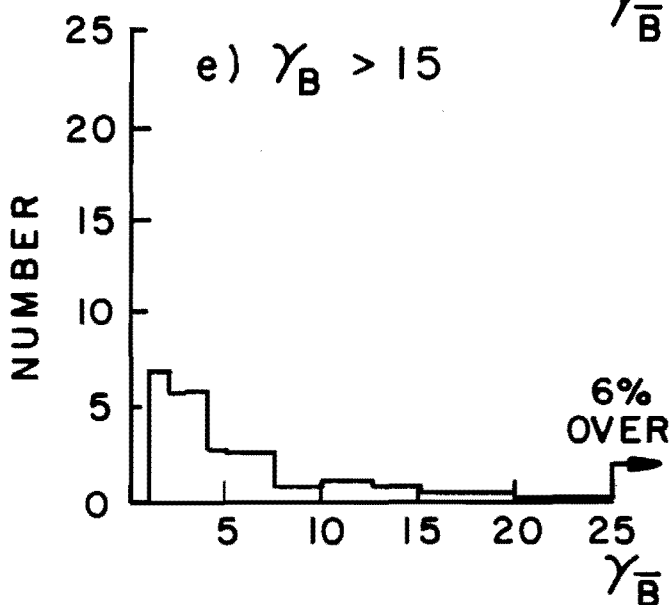
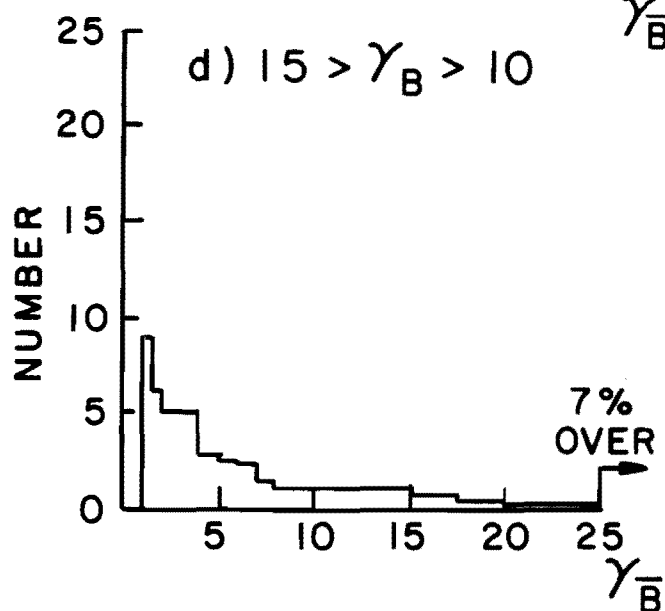
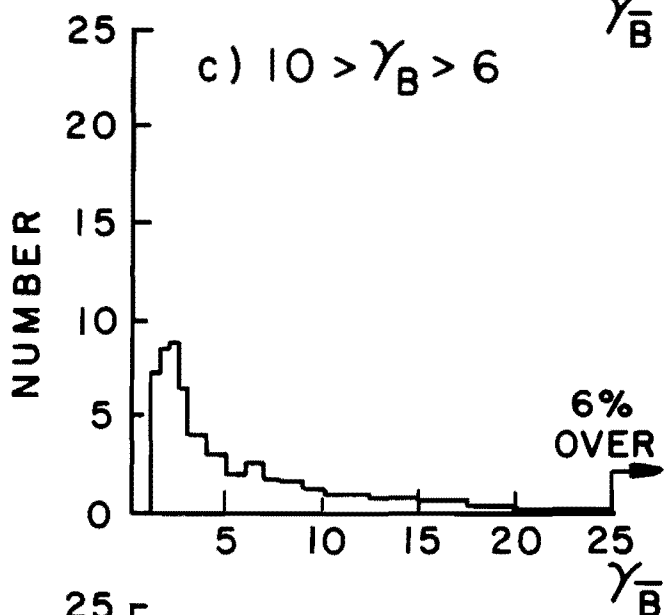
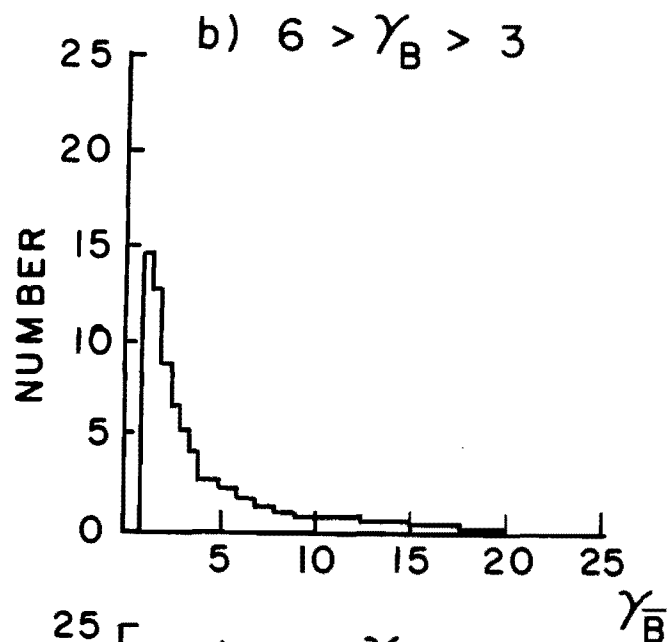
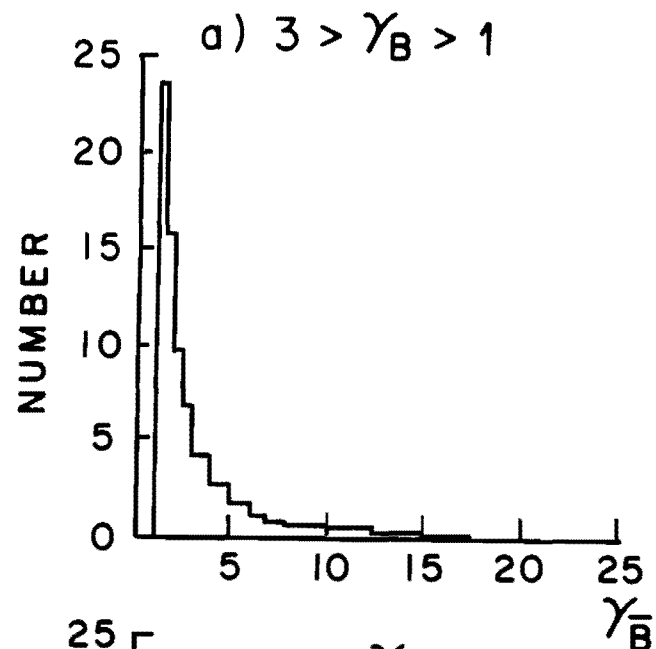


Figure 6 Gamma distributions (normalized to the same area) for an associated Beauty particle when the first Beauty particle has a gamma in the range specified below:

- a) $3 > \text{first gamma} > 1.$
- b) $6 > \text{first gamma} > 3.$
- c) $10 > \text{first gamma} > 6.$
- d) $15 > \text{first gamma} > 10.$
- e) $\text{first gamma} > 15.$

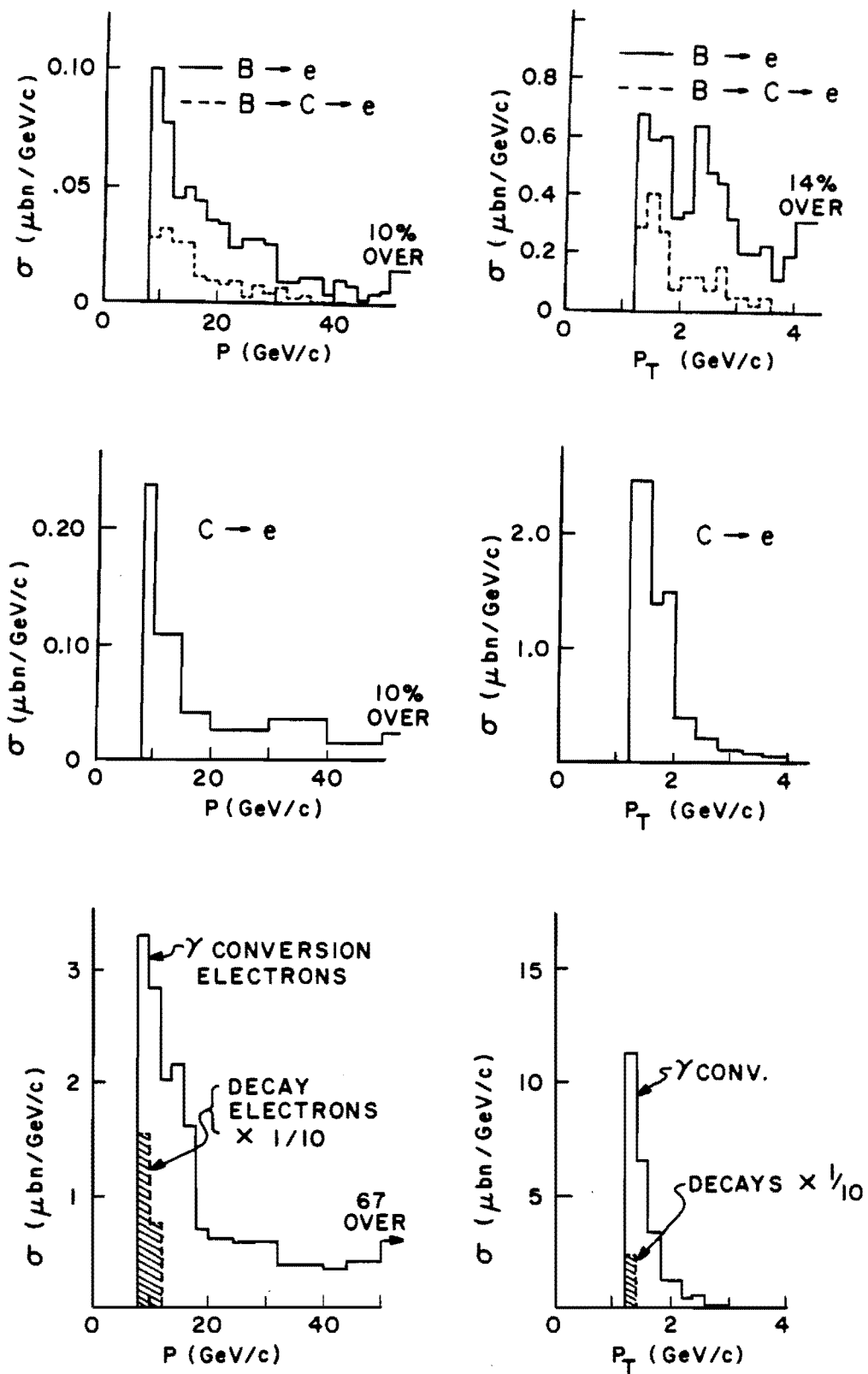


Figure 7 Momentum and transverse momentum for electrons satisfying $P > 8$ GeV/c and $P_T > 1.2$ GeV/c. P_T is figured with respect to the beam lines.

- a) For electrons from $B \rightarrow e$ and $B \rightarrow C \rightarrow e$ decays.
- b) For electrons from $C \rightarrow e$ decays.
- c) For background event electrons resulting from pion and kaon decays or 1% conversion of gamma rays.

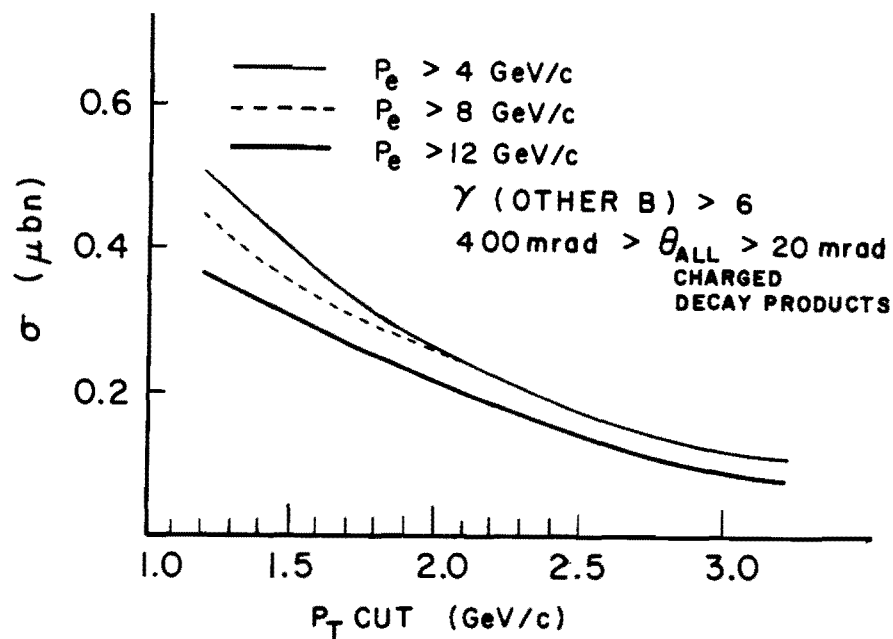


Figure 8 The yield of Beauty as a function of the PT of the tagging electron for events in which the tagging electron and all charged decay products from an accompanying B (with a $\gamma > 6$) are contained between production angles of 20 and 400 milliradians. The electron is assumed to have a momentum greater than 8 GeV/c.

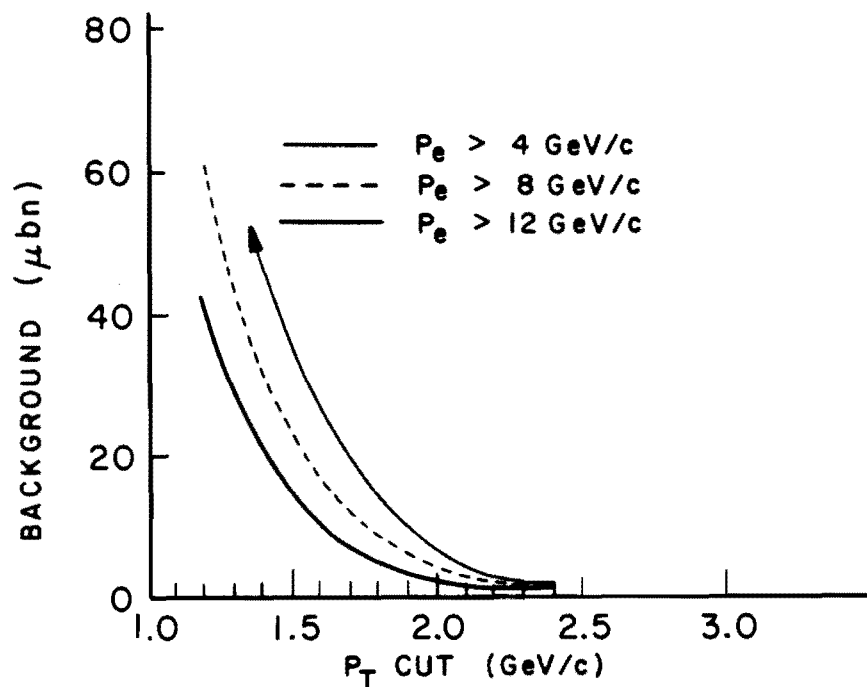


Figure 9 The electron trigger rate resulting from background events. For PT greater than 1.4 GeV/c it is entirely dominated by the assumed 1% gamma conversion.

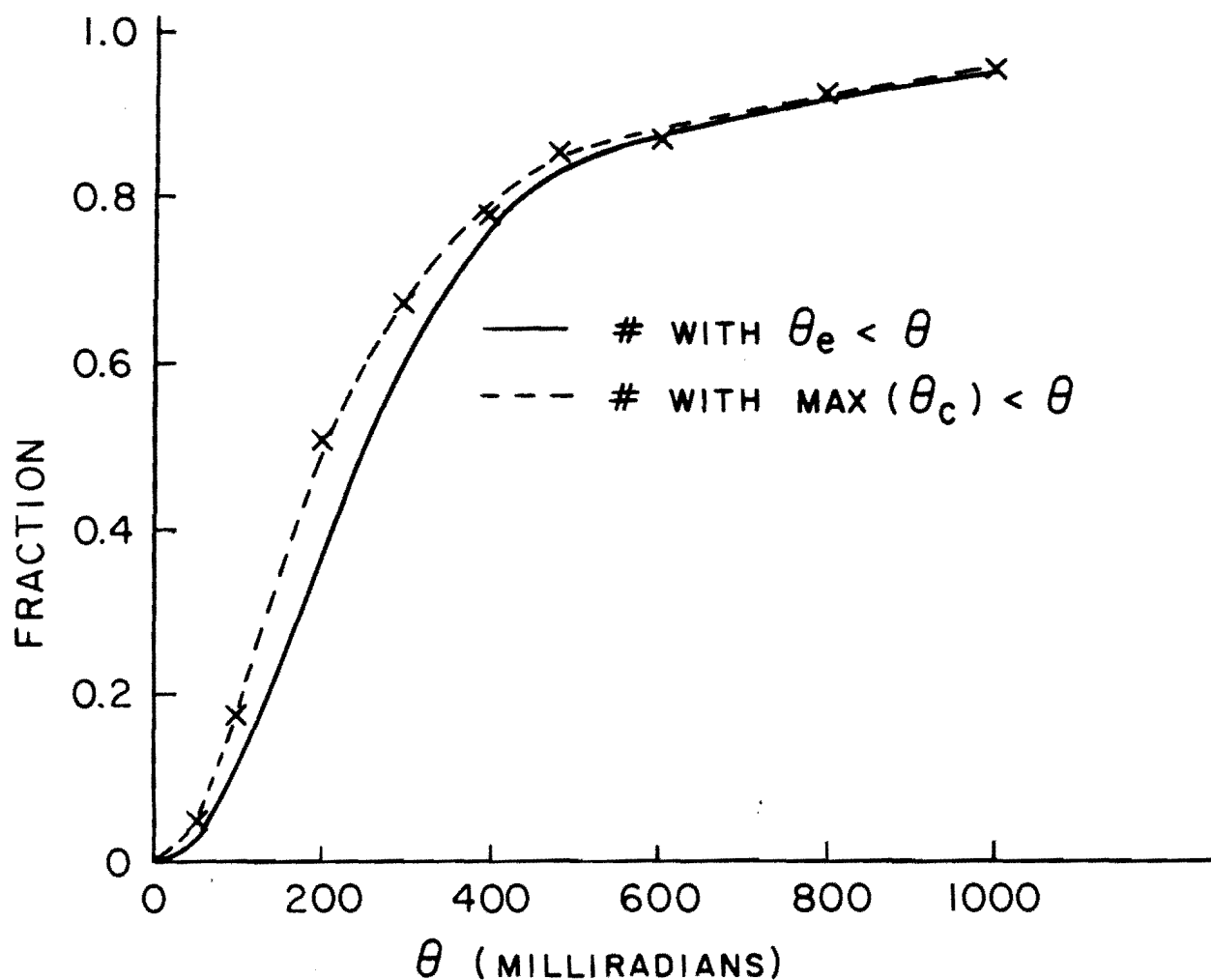


Figure 10 The fractional number of events in which the trigger electron is contained within an angle θ , and also the fractional number of events where all charged tracks from the associated Beauty decay (the one not giving rise to the electron trigger) are included within the specified angle.

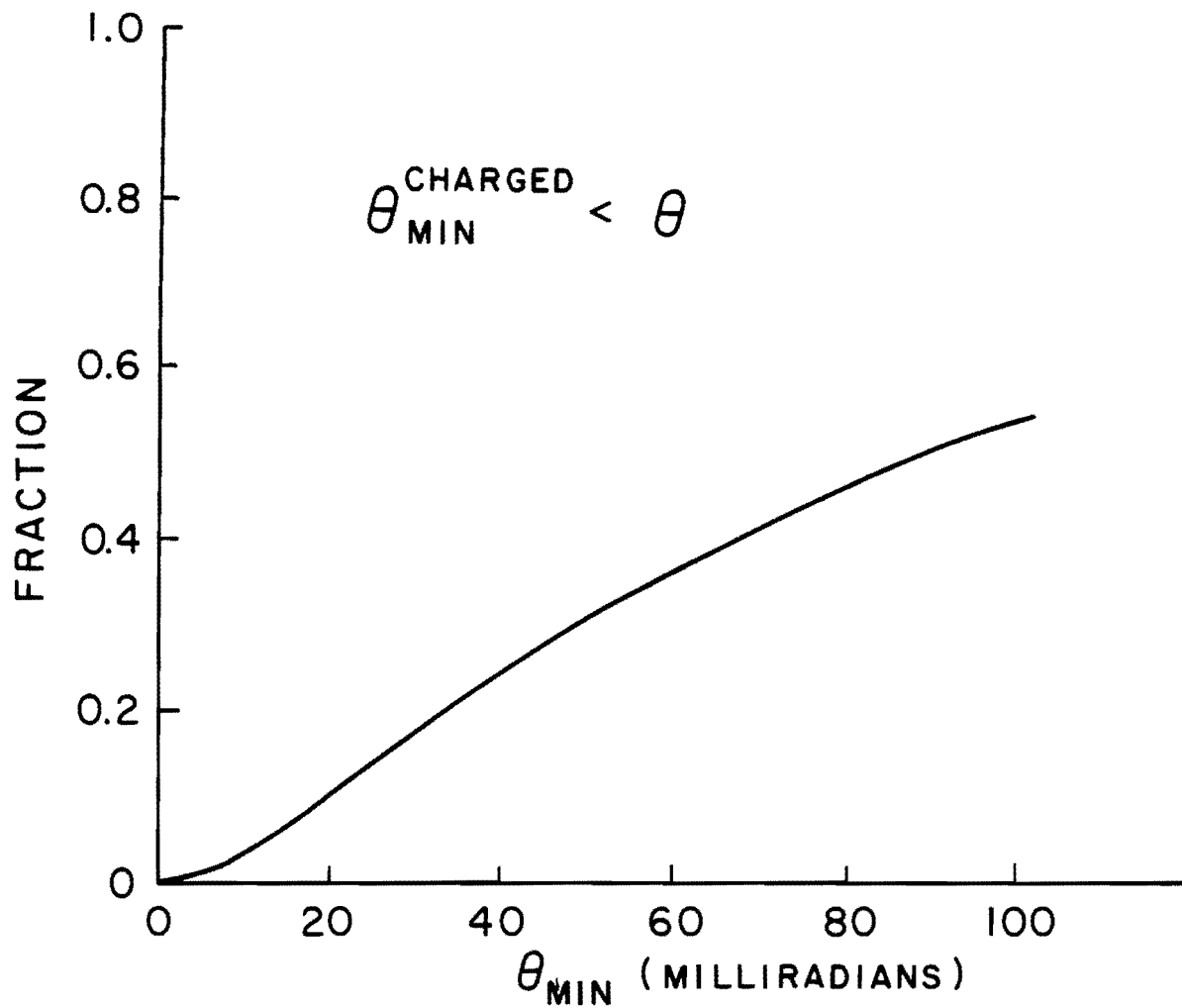


Figure 11 The fractional number events in which at least one charged track from the "other" Beauty decay has an angle less than theta. This gives an idea of how much is lost through the hole in the detector for the beams.

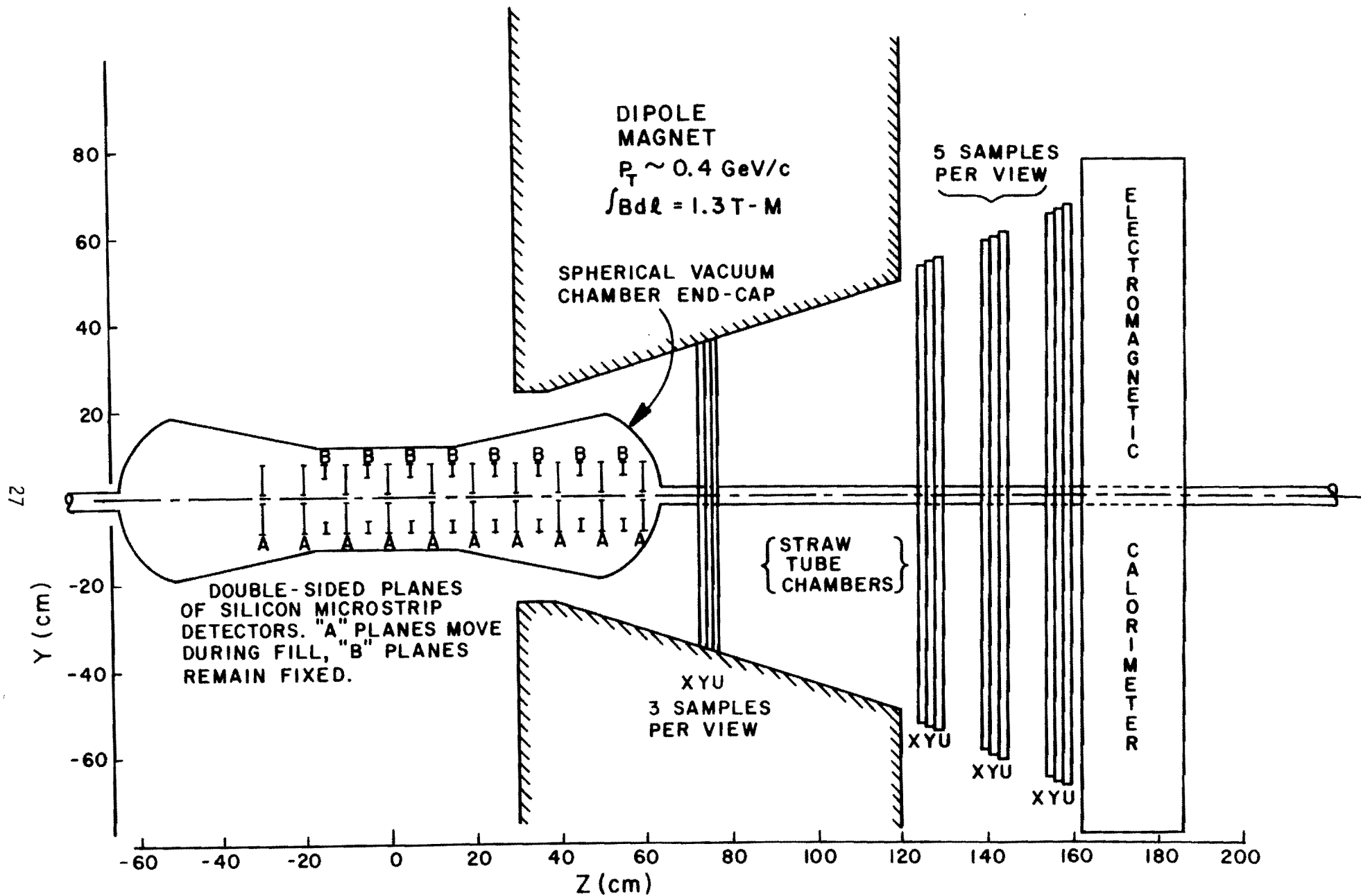


Figure 12 Elevation view of apparatus.